
AFRL-RI-RS-TR-2014-250

# RADIOMETRIC MEASUREMENTS OF SLANT PATH ATTENUATION IN THE V/W BANDS

*SEPTEMBER 2014*

INTERIM TECHNICAL REPORT

***APPROVED FOR PUBLIC RELEASE; DISTRIBUTION UNLIMITED***

STINFO COPY

**AIR FORCE RESEARCH LABORATORY**
**INFORMATION DIRECTORATE**

■ **AIR FORCE MATERIEL COMMAND** ■ **UNITED STATES AIR FORCE** ■ **ROME, NY 13441**

# NOTICE AND SIGNATURE PAGE

Using Government drawings, specifications, or other data included in this document for any purpose other than Government procurement does not in any way obligate the U.S. Government. The fact that the Government formulated or supplied the drawings, specifications, or other data does not license the holder or any other person or corporation; or convey any rights or permission to manufacture, use, or sell any patented invention that may relate to them.

This report was cleared for public release by the 88th ABW, Wright-Patterson AFB Public Affairs Office and is available to the general public, including foreign nationals. Copies may be obtained from the Defense Technical Information Center (DTIC) (http://www.dtic.mil).

AFRL-RI-RS-TR-2014-250 HAS BEEN REVIEWED AND IS APPROVED FOR PUBLICATION IN ACCORDANCE WITH ASSIGNED DISTRIBUTION STATEMENT.

FOR THE DIRECTOR:

**/ S /**
RICHARD MICHALAK, Chief
Information Transmission Branch

**/ S /**
MARK H. LINDERMAN
Technical Advisor, Computing
& Communications Division
Information Directorate

This report is published in the interest of scientific and technical information exchange, and its publication does not constitute the Government's approval or disapproval of its ideas or findings.

# REPORT DOCUMENTATION PAGE

*Form Approved*
**OMB No. 0704-0188**



| 1. REPORT DATE *(DD-MM-YYYY)* | 2. REPORT TYPE | 3. DATES COVERED *(From - To)* |
|---|---|---|
| SEPTEMBER 2014 | INTERIM TECHNICAL REPORT | AUG 2012 – APR 2014 |

**4. TITLE AND SUBTITLE**

RADIOMETRIC MEASUREMENTS OF SLANT PATH ATTENUATION IN THE V/W BANDS

**5a. CONTRACT NUMBER**
IN-HOUSE

**5b. GRANT NUMBER**
N/A

**5c. PROGRAM ELEMENT NUMBER**
62788F

**6. AUTHOR(S)**

George Brost, Kevin Magde, William Cook

**5d. PROJECT NUMBER**
T2WB

**5e. TASK NUMBER**
IN

**5f. WORK UNIT NUMBER**
HO

**7. PERFORMING ORGANIZATION NAME(S) AND ADDRESS(ES)**

Air Force Research Laboratory/RITE
525 Brooks Road
Rome NY 13441-4505

**8. PERFORMING ORGANIZATION REPORT NUMBER**

**9. SPONSORING/MONITORING AGENCY NAME(S) AND ADDRESS(ES)**

Air Force Research Laboratory/RITE
525 Brooks Road
Rome NY 13441-4505

**10. SPONSOR/MONITOR'S ACRONYM(S)**
AFRL/RI

**11. SPONSOR/MONITOR'S REPORT NUMBER**
AFRL-RI-RS-TR-2014-250

**12. DISTRIBUTION AVAILABILITY STATEMENT**

Approved for Public Release; Distribution Unlimited. PA# 88ABW-2014-1780
Date Cleared: 17 Apr 2014

**13. SUPPLEMENTARY NOTES**

**14. ABSTRACT**

Slant path brightness temperatures were measured at 72.5 and 82.5 GHz with a multi-channel radiometer. One year of measurements collected at 36 degree elevation angle in Rome, NY were examined in terms of attenuation statistics. A model-based attenuation retrieval algorithm was developed to determine the slant path attenuation cumulative distribution function to over 20 dB of attenuation corresponding to less than 1% exceedance probability. Slant path attenuation was also measured with the radiometer using the sun as a source of radiation. Over 30 dB of attenuation dynamic range was possible with this technique. Sun-beacon measurements were used to test model predictions.

**15. SUBJECT TERMS**

Radio propagation, attenuation, V-band, W-band, radiometer, radiative transfer

| 16. SECURITY CLASSIFICATION OF: | | | 17. LIMITATION OF ABSTRACT | 18. NUMBER OF PAGES | 19a. NAME OF RESPONSIBLE PERSON |
|---|---|---|---|---|---|
| a. REPORT | b. ABSTRACT | c. THIS PAGE | | | **KEVIN MAGDE** |
| U | U | U | UU | 9 | 19b. TELEPHONE NUMBER (*Include area code*) **N/A** |

# Radiometer Based Measurements of Slant-Path Attenuation in the V/W Bands

G. Brost, K. Magde, and W. Cook
Air Force Research Laboratory,
525 Brooks Rd, Rome, NY, USA
george.brost@us.af.mil

***Abstract*—Slant path brightness temperatures were measured at 72.5 and 82.5 GHz with a multi-channel radiometer. One year of measurements collected at 36° elevation angle in Rome, NY were examined in terms of the attenuation statistics. A model-based attenuation retrieval algorithm was developed to determine the slant path attenuation cumulative distribution function to over 20 dB of attenuation corresponding to less than 1% exceedance probability. Slant path attenuation was also measured with the radiometer using the sun as a source of radiation. Over 30 dB of attenuation dynamic range was possible with this technique. Sun-beacon measurements were used to test model predictions.**

***Keywords-radio propagation, attenuation, V-band, W-band, Radiometer, radiative transfer.***

## I. INTRODUCTION

The V/W satellite communication bands of 71-76 GHz downlink and 81-86 GHz uplink are attractive due to the available spectrum and large bandwidth. Reliable attenuation prediction capabilities are needed in order to analyze the utility and design requirements of a V/W satellite communications system. Extrapolation of existing models based on low frequency attenuation statistics has significant uncertainty[1,2]. There are currently no slant path attenuation statistics at the V and W bands with which to validate or develop propagation models. Radiometers offer the possibility to obtain the much needed attenuation statistics, albeit with certain limitations. Our goal is characterize V and W band attenuation to greater than 20 dB. In this paper we present 1 year of slant path attenuation statistics and analysis of the measurements made utilizing a four-channel radiometer.

The brightness temperature measurement of a radiometer can be related to the path attenuation $A$ (dB) along the direction of the antenna main beam [3,4] by

$$= 10 \log\left(\frac{T_{mr}-2.73}{T_{mr}-T_b}\right), \quad (1)$$

where $T_{mr}$ is the effective radiating temperature. For attenuation levels less than about 10 dB an approximate value of $T_{mr}$ is often sufficient to provide a good estimate of the attenuation [5]. Estimates of $T_{mr}$ can be determined from the surface meteorological data [6]. For higher levels of attenuation more accurate values of $T_{mr}$ are required due to the nonlinear behavior of equation (1) when $T_b$ is close to $T_{mr}$. The usual estimates of $T_{mr}$ based on radiosonde data are no longer reliable under these attenuating conditions. The problem is that $T_{mr}$ is a function of the unknown atmosphere that is being sensed and can be quite different than the climatic average.

A way to improve attenuation retrieval accuracy is with a model based approach in which the radiative transfer equation (RTE) is solved to calculate radiometer brightness temperature for representative model atmospheres. Hornbostel et al. [7] and Marzano [8] have demonstrated the efficacy of this approach by comparing their predictions with beacon data. We also adopt a model-based approach to retrieve the attenuation from brightness temperature measurements.

## II. EXPERIMENTAL

Radiometric data was collected in Rome, NY (43.2° N, 75.4°W). The radiometer used in our experiments was a four channel liquid water profiler with receivers at 23.8, 31.4, 72.5 and 82.5 GHz. The four channels of the RPG model LWP-U72-U82 radiometer share a common parabolic antenna of 30 cm diameter. The antenna is protected by a radome and has a heated blower to mitigate affects due to hydrometeors. Brightness temperature resolution of the radiometer is better than 0.2 K at 1 second integration time.

An experimental technique to measure V/W band attenuation uses the sun as a source of V and W band radiation. Objectives of the sun-beacon measurements are to validate model results and/or empirically determine an attenuation retrieval algorithm. The sun can be modeled as a uniform disk of 32 minutes of arc [9]. The brightness temperature of a radiometer pointing at the sun is given by

$$T_b = T_A + T_S e^{-\tau} \quad , \quad (2)$$

where $T_A$ is the brightness temperature due to the atmosphere, $\tau$ is the opacity of the atmosphere, and $T_S$ is the contribution from the sun in the absence of any atmospheric attenuation. Examples of brightness temperature measurements made by scanning the radiometer across the sun are shown in Figure 1. In the switching experiment two measurements are made; one measurement pointing at the center of the sun, the other pointing off the sun. The difference is $T_S e^{-\tau}$. $T_S$ depends on

frequency and beamwidth and can be determined from measurements taken in clear weather. The scan steps of the radiometer were 0.1° in azimuth and 0.1° in elevation. The standard deviation of $T_S$ was less than 2% for 72.5 and 82.5 GHz and less than 1% for 23.8 and 31.4 GHz. Over 30 dB of dynamic range in path attenuation measurement is possible at V and W bands with this technique. An Example of attenuation measurements made during a rain event is shown in Figure 1. These measurements were made at elevation angles between 30° and 36°. The background measurements were made at 5° offset from the sun to accommodate the larger beamwidths at the lower frequencies.

The main source of error in this approach is due to the spatial variation of the atmosphere and the difference between the background measurement made pointing off the sun and that made pointing at the sun. The spatial variation is a source of the scatter in the data. This is quantified by measurements of the spatial structure made by scanning the radiometer in azimuth. It is expected that the spatial inhomogeneity will mostly result in scatter about the true attenuation with some small number of larger deviations.

## III. Attenuation Retriveal Methodology

The approach to retrieve attenuation was to relate the V and W band attenuation to the available measured observables of radiometer brightness temperature and surface temperature ($T_S$), pressure ($P_S$) and relative humidity ($RH_S$). Attenuation derived from equation (1) with a $T_{mr}$ that was a function of $T_S$, $P_S$, and $RH_S$ was assumed valid for A < 10 dB. For higher levels of attenuation a model-based retrieval algorithm was applied. The methodology was to apply a statistically representative model of the atmospheric conditions and calculate the vector $A(T_b,T_S,P_S,RH_S,R)$ that related the attenuation to the measured observables and an atmosphere that was parameterized by the rain rate $R$. The main assumption guiding the radiometric modeling was that the 72.5 and 82.5 GHz slant-path attenuation statistics could be satisfactorily determined with an attenuation model that was descriptive of widespread stratiform rain. With the high rain specific attenuation at these frequencies attenuation levels could exceed

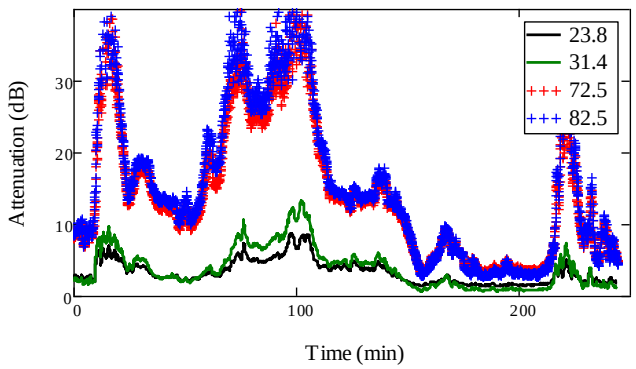


Figure 1. Attenuation measured with sun-beacon .

20 dB with rainfall rates of only a few mm/hr at the 36° elevation angle used. This does not mean that convective rain did not contribute to attenuation. The assumption was that the attenuation statistics at these levels were dominated by stratiform rain and neglecting convective rain had little impact on the statistics.

An atmospheric model based on radiosonde data was developed that described the altitude dependence of temperature, pressure, and water vapor as a function of the surface conditions for Rome NY. A rainy atmosphere was imposed on the background atmosphere. The rain model included a melting layer and clouds which were parameterized to the rainfall rate. Here we assumed that the rain and other hydrometeors were horizontally stratified.

The rain field was assumed to be uniform and the rain height determined by the freezing level. If no melting layer was present, the rain height was set equal to the 0˚C isotherm. If the melting layer was present then the rain height was set equal to the bottom of the melting layer. Rain drop size distributions (DSD) were assumed to be described by the gamma DSD:

$$N(D) = N_0 D^{\nu} e^{-\Lambda D} , \qquad (3)$$

where N is the differential number density and the coefficient $N_0$ and slope parameter $\Lambda$ may be functions of the rain rate. The Marshal-Palmer [10] rain DSD was considered to be most representative of stratiform rain. As polarization effects were not considered the extinction and scattering parameters for the rain were determined from Mie scattering theory. The temperature of rain was taken to be the wet bulb temperature. We assumed the atmospheric relative humidity to be 90%, which resulted in a rain temperature about 1K below the atmospheric temperature.

A melting layer model was derived from analysis of calculated radiative properties based on melting model formulation of Szyrmer and Zawadzki [11]. Melting layer predictions depend on the assumed parameters of snow density, particle velocities, and dielectric model. An example of melting layer characteristics for 72.5 GHz for a rain rate of 5 mm/hr is shown in Figure 2. Here we assumed a snow density of 0.1 g/cm and a three component mixture dielectric model. The radiative properties were calculated for spherical particles. The melting layer model implemented for this study was based on a sensitivity analysis to model parameter variations. The melting layer was taken to be 400 m thick with averaged radiative parameters which depended on the rain rate. The extinction coefficient was about 1.5 times the extinction of the rain and the average scattering albedo and asymmetry parameter increased by about factor of two over the rain values.

The cloud liquid water path was determined from rain height and rain rate through the relation proposed by Wentz and Spencer [12]

$$LWP = .18\left(1 + \sqrt{H_R R}\right) . \qquad (4)$$

Here LWP is in kg/m$^2$ when $H_R$ is in km and $R$ is in mm/hr. A uniform cloud below the zero degree isotherm was assumed. This model resulted cloud liquid water contents generally less than 1 gm$^{-3}$ and in attenuations up to a few dB. The LWP determined by equation (4) was mapped onto the measured rain

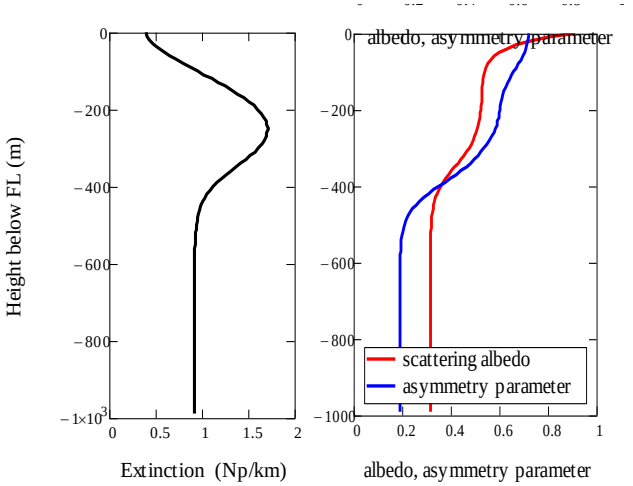


Figure 2 Melting layer characteristics for 72.5 GHz, at R = 5 mm/hr.

rate cumulative distribution function (CDF) with an average rain height of 3.9 km and compared with the cloud LWP CDF predicted by the ITU R. P840 model [13], which was derived from reanalysis of numerical weather models. The calculated LWP was about one half of that predicted by the ITU cloud model for the same time percentages. The cloud model LWP is statistically representative though the correlation with rain is an assumption.

The snow region above the melting layer is a potential source of attenuation for the V and W bands and was included in the rain model. This a region of about 1 to 2 km in which the ice particles aggregate to form large irregularly shaped snowflakes. The melting layer model assumption of constant mass flux means that the liquid equivalent snow fall rate at the top of the melting layer should be the same as the rainfall rate. To model the radiative characteristics of the snow cloud we have assumed that the average snow extinction was related to the rain rate by a power law relation

$$ks_e = \alpha R^{\beta} \ (\mathrm{km}^{-1}), \qquad (5)$$

where $\beta \approx 1$ and $\alpha$ is a frequency dependent parameter. Determination of $\alpha$ is uncertain as there is little experimental data and theoretical values depend on model assumptions. The measurements by Li et al. [14] and the analysis by Heymsfield et al. [15] both indicated a specific attenuation of about 0.2 dB/km at 94 GHz at for a rain rate of about 4 mm/hr. We take $\alpha = 0.012$ (hr/m$^2$) and $\beta = 1$ at 94 GHz and scale to other frequencies resulting in a value of 0.007 at 72.5 GHz and .009 at 82.5 GHz. Terrestrial measurements of snow attenuation [16,17] and an earlier analysis by Matrosov [18] using a different snow density function suggest a somewhat greater extinction coefficient. The scattering albedo was taken to be 0.92 and the asymmetry parameter was taken to be 0.6. The snow layer depth was set at 1.5 km.

A Monte-Carlo simulation which allowed three dimensional photon trajectories was used to solve the radiative transfer equation (RTE) for scattering atmospheres. Photons were launched from the radiometer and traced backwards to their source of emission. The scattering phase function was determined from the asymmetry parameter $g$. If $g$ was greater or equal to 0.2 the phase function was approximated by the Henyey–Greenstein phase function [19]. If g was less than 0.2 a combined Henyey-Greenstein and Rayleigh phase function proposed by Liu and Weng [20] was used. The ground was assumed to be at the same temperature as the surface temperature with an emissivity of 0.95 and Lambertian phase function. The radiometer brightness temperature was calculated for different conditions within the framework of this atmospheric model.

As our focus was on attenuation retrieval we evaluate the dependence of attenuation on brightness temperature (A-$T_b$). A sensitivity analysis examined the effects of various parameters and model assumptions.

V and W band attenuation and scattering characteristics are sensitive to the rain DSD. As the rain DSD and its variability had not been measured for this location, the Marshall-Palmer (M-P) DSD was considered to be statistically representative of stratiform rain. Figure 3 compares A-$T_b$ for the M-P and the Laws-Parsons (L-P) [21] and Joss-Thunderstorm (J-T) [22] DSDs and a surface temperature of 20°C. Figure 3 also shows the case for an M-P DSD with the scattering albedo set to zero.

The atmospheric model used the average zero degree isotherm height correlated with surface temperature as the rain height.. However there is significant variation in the freezing level with standard deviation about the mean of about 1 km. The effect of rain height variability is shown in Figure 4 which compares the A-$T_b$ for different rain heights with a surface temperature of 20°C. Although attenuation and brightness temperature depended on rain height for a given rain rate, the rain height only weakly affected the attenuation-brightness temperature curves. Similar results were observed for variations in melting layer extinction and cloud LWC, depth, and height. The attenuation–brightness temperature characteristics were not changed much by modest variations (factors of up to 2 or 3) in the relevant parameters. The A-$T_b$ dependence on surface temperature is shown in Figure 5.

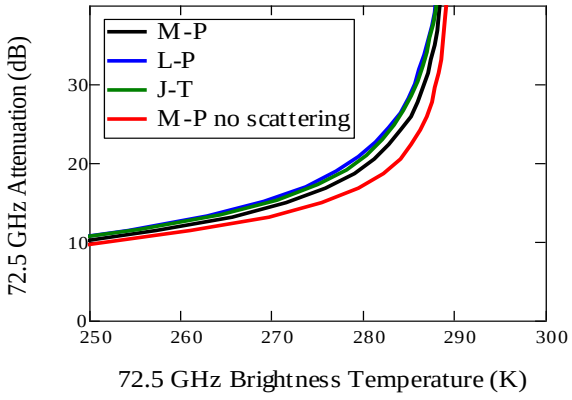


Figure 3. Calculated 72.5 GHz attenuation vs brightness temperature for different rain DSDs.

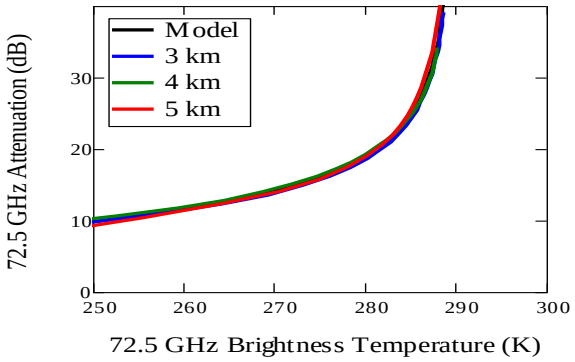


Figure 4 Calculated 72.5 GHz attenuation vs brightness temperature for different rain heights.

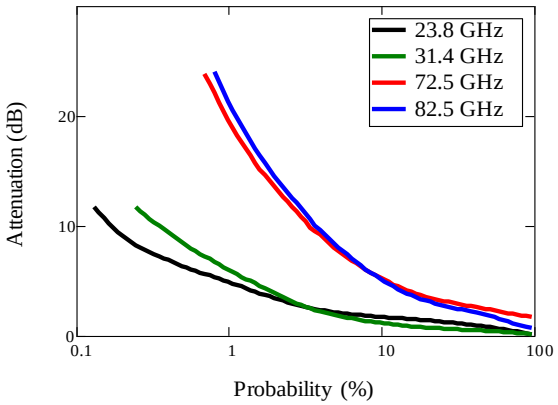


Figure 6. Measured attenuation statistics for Rome, NY.

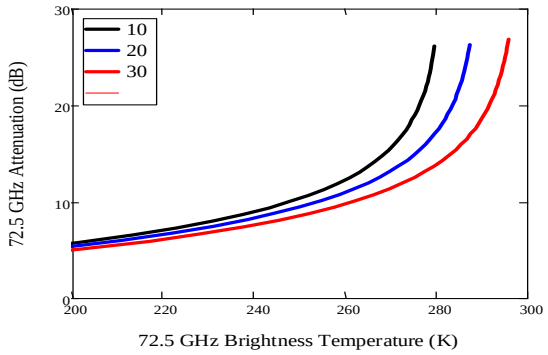


Figure 5. Calculated 72.5 GHz attenuation vs brightness temperature for different surface temperatures.

## IV. Results and Anlysis

The results of the sensitivity analysis showed that the attenuation-brightness temperature characteristics were quite robust to most of the model parameters. Consequently an attenuation retrieval algorithm could be implemented by relating the attenuation to brightness temperature and surface temperature for an assumed rain DSD. Figure 6 shows the retrieved attenuation statistics for the four frequency channels assuming a Marshall-Palmer DSD. The V and W band results exhibit a small shift around 10 dB due to the use of equation (1) for attenuation less than 10 dB.

We consider next some of the sources of error and uncertainty in the attenuation statistics. Figure 7 compares the attenuation statistics at 72.5 GHz derived for the three different rain DSDs; Marshall-Palmer (MP), Laws-Parsons (LP), and Joss-thunderstorm (JT). The choice of DSD did not have a strong impact on the attenuation statistics. The attenuation retrieval algorithm was based on a point measurement of surface temperature. Temperature variability over the slant path was not measured. Figure 8 shows the variation in attenuation statistics for +/- 1°K from the assumed temperature. Within the context of the atmospheric model, this appears to be the largest source of uncertainty.

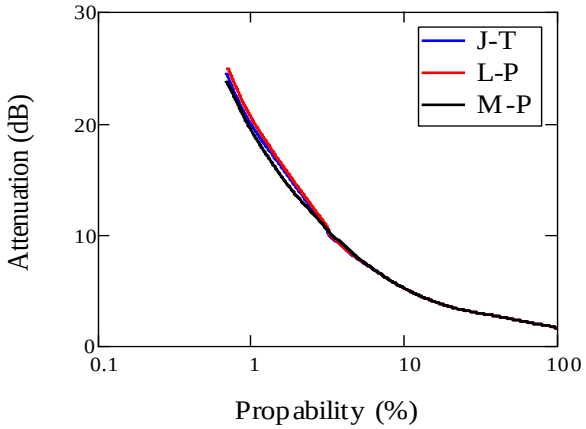


Figure 7 Comparison of attenuation statistics at 72.5 GHz for different rain drop size distributions.

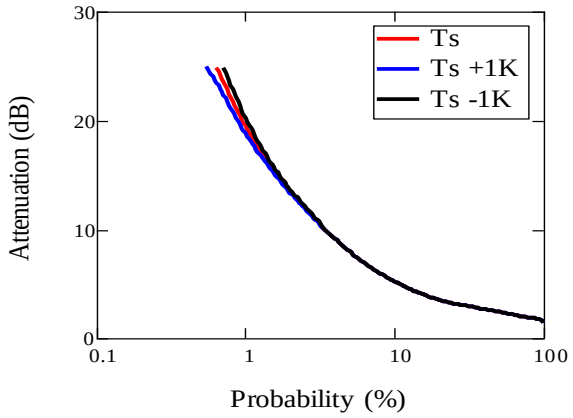


Figure 8 Surface temperature sensitivity of attenuation retrieval algorithm for 72.5 GHz.

The attenuation retrieval model assumed that neglecting the occurrence of finite rain cells had little impact on the retrieved attenuation statistics for the relevant time percentages. To quantitatively test the validity of this assumption we compared the A-$T_B$ calculated for a slant path (36° elevation angle) between a model of wide-spread rain and a rain cell model that included rain cell size characteristics. The concept was to estimate the statistical occurrence of convective rain cells in the radiometric data by relating their occurrence to the measured rain rate statistics. For this analysis it was convenient to assume uniform cylindrical (or square) rain cells imbedded in large area of stratiform rain. The top-hat model was adopted from that of Misme and Waldtuffle [23] in which the rain rate in the plateau region was related to the cell rain rate by

$$R_p = 10[1 - e^{-0.0105R}] \text{ (mm/hr)} \qquad (6)$$

The measured rain rate statistics were used to calculate the rain rate CDF for a specified exceedance attenuation *A*, rain height $H_R$, and rain cell diameter D(R). This CDF represented the distribution of rain rates that could produce an attenuation that exceeded *A*. The three-dimensional Monte Carlo radiative transfer simulation calculated the brightness temperature and attenuation for rain rates drawn from the CDF. Attenuation from clouds and melting layer were not included in this analysis. The spatial location of the rain cell center was determined by random draw from the corresponding spatial area determined by A, $H_R$, D(R) assuming equal probability. Different models that related rain cell size to rain rate were examined. An example calculation is shown in Figure 9 for a rain cell model given by

$$Dia(R) = 27R^{-.54} \text{ (km)} \qquad (7)$$

and 12 C surface temperature. Scatter in the data points increased with surface temperature and depended also on the particular rain cell size model. The main conclusion of this analysis was that the uniform/ widespread rain model was most likely to under-estimate the attenuation by a few percent.

We considered the use of the K-band frequencies in the attenuation retrieval but found it to be of limited value. While the V and W band A-$T_b$ did not depend strongly on the model parameters, the V and W band attenuation relationships to the K-band brightness temperatures and attenuations were much more sensitive to model assumptions.

The attenuation retrieval algorithm was tested against Sun-beacon data shown in Figure 1. In the Sun-beacon mode half the data collected corresponds to the radiometer pointing off the Sun. The retrieval algorithm was applied to these brightness temperatures. The surface temperature varied between 12 and 13 C and the elevation angle varied from 30 to 36°. The measured rain rate near the radiometer was typically a few mm/hr with a peak of 15 mm/hr. Radar data was not available to confirm the existence of a bright band, but this most like a stratiform rain event. Figure 10 compares the 72.5 GHz. model predictions with the 72.5 GHz measured attenuation.

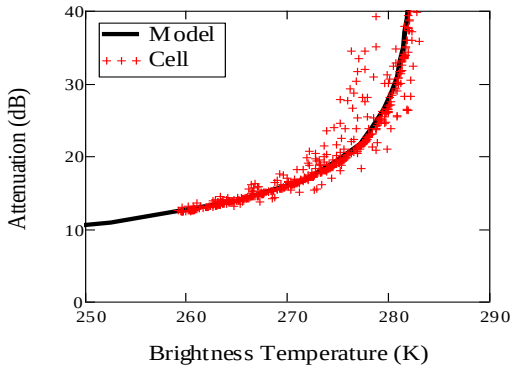


Figure 9. Comparison of the uniform/widespread rain model with a finite cell model that incorporated the rain cell statistics.

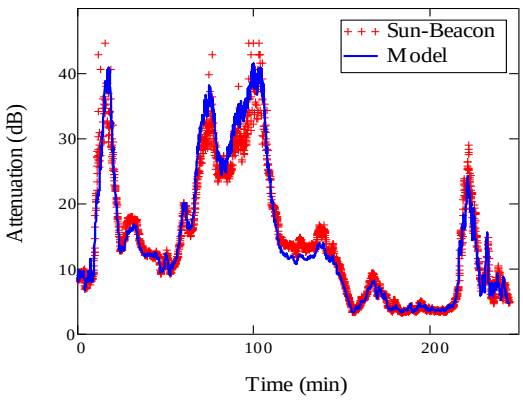


Figure 10. Comparison of model predictions with Sun-Beacon attenuation measurements.

## V. SUMMARY

This paper presented radiometer based slant path attenuation measurements and analysis. Slant path brightness temperatures were measured in the V/W bands at 72.5 and 82.5 GHz as well as 23.8 and 31.4 GHz with a multi-channel radiometer. Attenuations up to 10 dB were calculated by equation (1) using a $T_{mr}$ that depended on simultaneous surface meteorological measurements. V and W band attenuations were extended to values greater than 20 dB with a model based retrieval. This model assumed uniform widespread rain. The argument for the validity of this model was that the V and W band attenuation statistics for exceedance probability in the range of 1 to 3% are dominated by stratiform rain. An analysis of finite rain cell sizes and statistics estimated that the error associated with this assumption would cause a slight under-estimation of attenuation. A sensitivity analysis showed that the attenuation dependence on brightness temperature was sensitive to surface temperature, but quite robust to other model parameters including rain height, melting layer, and cloud content. This allowed an attenuation retrieval algorithm that related attenuation to surface temperature and brightness temperature. A sun-beacon technique to measure slant path attenuation with over 30 dB of dynamic range using the radiometer was described. Comparison of the statistical model with the instantaneous Sun-beacon data showed good agreement. These are the first measurements of slant path statistics at frequencies above 50 GHz.

## REFERENCES


[1] G. Brost, W. Cook, and W. Lipe," On the modeling and prediction of Attenuation for V/W Satellite Communications", Ka and Broadband Communications Conference, Palermo, 2011.

[2] G.A Brost,. W.G. Cook, "Analysis of empirical rain attenuation models for satellite communications at Q to W band frequencies", 6th European Conference on Antennas and Propagation (EUCAP), 2012, 10.1109/EuCAP.2012.6205935, pp. 1455-1459.

[3] S. Chandrasekhar, Radiative Transfer, Dover Publications, New York, 1960.

[4] G. Brussaard, "Radiometry - a useful prediction tool?", ESA SP-1071, EDA, Paris, 1984.

[5] R.M. Allnutt, T. Pratt, W.L. Stutzman, and J.B. Snider, "Use of radiometers in atmospheric attenuation measurments", IEE Proc. Microw. Antennas Propag. Vol 141, 428-432, 1994.

[6] J.C. Liljegren, E.E. Clothiaux, G.G. Mace, S. Kato, and X. Dong, " A new retrieval for cloud liquid water path using a ground-based microwave radiometer and measurements of cloud temperature", J. Geophys. Res. vol 106, pp 14485-14500, 2001.

[7] Hornbostel A. and Schroth A. and Kutuza B. (1994), "Polarimetric Measurements and model measurements of downwelling rain brightness temperature", Proceedings of μrad94, Rome, Italy.

[8] F. S. Marzano, "Predicting antenna noise temperature due to rain clouds at microwave and millimeter-wave frequencies," IEEE Trans. Antennas and Propagat., vol. 55, n. 7, pp. 2022-2031, 2007

[9] D.L. Croom, "Sun as a broadband source for tropospheric attenuation measurements at millimetre wavelengths", Proc. IEE, vol 120, 1200-1206, 1973

[10] J. Marshall and W. Palmer , "The distribution of raindrops with size", Journal Meteorology, vol 5, pp 165-166, 1948.

[11] W. Szyrmer and I. Zawadzki, "Modeling of the melting layer: Part I. Dynamics and microphyics", J. Atmos. Sci. vol 56, 3573-3592, 1999.

[12] F.J.Wentz and R.W. Spencer, "SSM/I rain tetrievals with a unified all – weather ocean algorithm", J. Atmos. Sci., 55, 1613-1627, 1998.

[13] International Telecommunication Union-Radiocommunication (ITU-R) (2013), Attenuation due to clouds and fog., *Recomm ITU-R P.840-6*, Geneva, Switzerland.

[14] L.Li, S.M. Sekelsky, S.C. Reising, C. T. Swift, S.L. Durden, G. A. Sadowy, S. J. Dinardo, F.K. Li, A. Huffman, G. Stephens, D.M. Babb, and H.W. Rsenberger, "Retrieval of atmospheric attenuation using combinded ground-based and airborne 95-GHz cloud radar measurements", J. Atmos. Oceanic Technol, 18, 1345-1353, 2001.

[15] A. J. Heymsfield, A. Bansemer, S. Matrosov, and L. Tian,"The 94-GHz radar dim bnad: Relevance to ice cloud properties and CloudSat", Geophys. Res. Lett., 35, L030802, doi: 10.1029/2007GL031361.

[16] H.B. Wallace,"Millimeter-wave propagation measurements at the Ballistic Research Laboratory", IEEE Tans. Geos. Remote Sens., vol 26, 253-258, 1988.

[17] J. Nemarich, R. J./ Wellman, and J. Lacombe, "Backscatter and attenuation by falling snow and rain at 96, 140, and 225 GHz.",

[18] S.Y. Matrosov, "Modeling backscatter properties of snowfall at millimeter wavelengths", J. Atmos. Sci. 64, 1727-1736, 2007.

[19] L. Henyey and J.Greenstein, "Diffuse radiation in the galaxy", Astrophys. J., vol 93, 79-83, 1941.

[20] Q. Liu and F. Weng, "Combined Henyey-Greenstein and Rayleigh phase function", Applied Optics, vol 45 pp7475-7479, 2006.

[21] J.O. Laws and D.A. Parsons, "The relation of raindrops-size to intensity", Trans. Amer. Georphys. Union, 24, 452-460, 1943.

[22] J. Joss, J.C. Thams, and A. Waldvogel, "The variation of rain-drop size distribuitons at Lacarno", in Proc. Internat. Conf. on Cloud Physics, 369-373, 1968.

[23] P. Misme and P. Waldteufel, " A model for attenuation by precipitation on microwave earth-space link", Radio Science, vol 15 pp. 655-665, 1980.